Highly Confined Flow Past a Stationary Square Cylinder

Shravan Kumar Mishra, Deepak Kumar, Kumar Sourav, Pavan Kumar Yadav and Subhankar Sen

Abstract Present work explores a numerical study based on Finite-Element Method for fluid flow past a stationary square cylinder placed symmetrically in the channel with high Blockage, $B = 0.9$. Reynolds Number (Re) progressively varied from 5 to 150 in the laminar region. An attention has been paid to capture the exact point of laminar flow separation on the surface of the cylinder and the separation Re for high blockage flow. The steady to unsteady flow transition is observed at a Re (Re_c) of 62. A very high drag coefficient, order of magnitude = 10^3 is reported for the computation. Inconsistency with unbounded flow solutions, the wake bubble for 90% blockage cylinder shows nonlinear variation with Re in the steady flow regime. In a very narrow regime near the beginning of unsteadiness, the flow is found to be quasi-periodic whereas, for all remaining Reynolds number values considered for the present study, periodic flow is observed.

Keywords Stabilized finite-element · Confined flow · High blockage

1 Introduction

Bluff body flow had been a widely explored research area for several decades. While a majority of earlier works used a circular cylinder to study the flow characteristics in both steady and unsteady conditions, knowledge of flow around other cross-sections lacked. The researchers have been trying to study the physics of the flow behind other cross-sections like a square, rectangle, ellipse, etc. Confining the flow significantly affect the flow characteristics around a bluff body. Owing to vast applications of confined flow (viz., flow in journal bearing, in the arteries of the

S. K. Mishra (✉) · D. Kumar · K. Sourav · P. K. Yadav · S. Sen
Department of Mechanical Engineering, Indian Institute of Technology (Indian School of Mines) Dhanbad, Dhanbad 826004, Jharkhand, India
e-mail: shravan.1992.mishra@gmail.com

P. Saha et al. (eds.), *Advances in Fluid and Thermal Engineering*,
Lecture Notes in Mechanical Engineering,
https://doi.org/10.1007/978-981-13-6416-7_12

human body, etc.), a number of studies had been and are being performed to study the effect of blockage on flow. Blockage (B), being an influential parameter, is the ratio of the characteristic dimension of an object across the flow to the width of the computational domain.

Unconfined and moderately confined flow had been studied vastly by researchers [1–5]. An interesting outcome from the above studies makes the platform for the need of study of highly blocked flow around an obstacle. For a square cylinder, [6] presented drag coefficients and Strouhal number for different cases in Re = [37.5, 150] and B = [0.05, 0.5] range. For a circular cylinder, [7] investigated wall effect up to high blockage ($0.1 \leq B \leq 0.9$) on two-dimensional (2D) flow ($0 < Re \leq 280$). They focused on hydrodynamic force range in the wake structure behind the cylinder. They reported pitchfork and supercritical Hopf bifurcation. In addition, the presence of co-dimension point on the neutral stability curve had also been reported. The existence of the steady asymmetric state and its transition due to pitchfork bifurcation was obtained by employing linear stability study. [8], for laminar flow (Re = [6–40]) and B = [0.00125, 0.80], around a stationary circular cylinder, reported the separation Re (Re_s) to be 6.29 (approximately) for 0.5% blocked flow. They also observed that the effect of blockage had negligible influence on the flow parameters for $B \leq 0.01$. The bubble length, separation angle, and Re_s exhibit monotonic variation with blockage. They were the first to present the variation of separation angle with Re. For a square cylinder at zero incidence, [9] performed direct numerical simulations (DNS) at different Re over a wide range of B between 10 and 90%. They noted that critical Re (Re_c) display a non-monotonic variation with increasing blockage as earlier reported by [3] for a square and [4] for a circular cylinder.

It is quite clear that there are not plenty of works available to wrap the physics of high blockage flow. Thus, in the present work, an attempt has been made to study the effect of high blockage on flow characteristics and fluid forces for flow around a square cylinder.

2 Governing Equations and Finite-Element Formulation

The momentum and mass conservation equations (Eqs. 1 and 2) govern the movement of an incompressible viscous fluid. The equations, in their vector form, using primitive variables are:

$$\rho(\partial \mathbf{u}/\partial t + \mathbf{u} \cdot \nabla \mathbf{u}) - \nabla \cdot \boldsymbol{\sigma} = 0 \tag{1}$$

$$\nabla \cdot \mathbf{u} = 0. \tag{2}$$

Here ρ, $\mathbf{u}$, t and $\boldsymbol{\sigma}$ are the fluid density, velocity field, time and the Cauchy stress tensor, respectively. The stress can further be described as the sum of its isotropic ($p\mathbf{I}$) and deviatoric parts ($\mathbf{T}$). Mathematically,

$$\sigma = p\mathbf{I} + \mathbf{T}; \quad \mathbf{T} = 2\mu\varepsilon(u); \quad \varepsilon(u) = \frac{1}{2}\left((\nabla u) + (\nabla u)^{\mathrm{T}}\right) \tag{3}$$

where p, $\mathbf{I}$, μ and ε are the pressure, identity tensor, dynamic viscosity of the fluid and strain rate tensor, respectively.

A stabilized finite-element method is employed to discretize the fluid flow equations (Eqs. 1 and 2). The discretized equations are solved iteratively over the co-allocated mesh. The use of co-allocated mesh violates the Babuska-Brezzi condition and hence involves the addition of extra stabilizing terms for velocity (SUPG: Streamline-Upwind/Petrov Galerkin) and pressure (PSPG: Pressure-Stabilized/Petrov Galerkin), respectively. Further details of the finite-element formulation can be found in [10, 11].

3 Problem Description

3.1 Computational Domain and Boundary Conditions

A square cylinder of dimension D is placed symmetrically between in a rectangular computational domain $PQRS$. The lateral walls are separated by a distance H; the width of the computational domain (here, $H = 1.1111D$). In Fig. 1, the set-up is shown for $B = 0.9$. The inlet is at a distance of $L_u = 32D$ behind the cylinder center while the exit is $L_d = 63D$ past the cylinder center. The origin of the Cartesian coordinate system coincides with the cylinder center.

A fully developed flow enters the channel and exits without stress. The lateral walls and cylinder surface are governed by the no-slip condition.

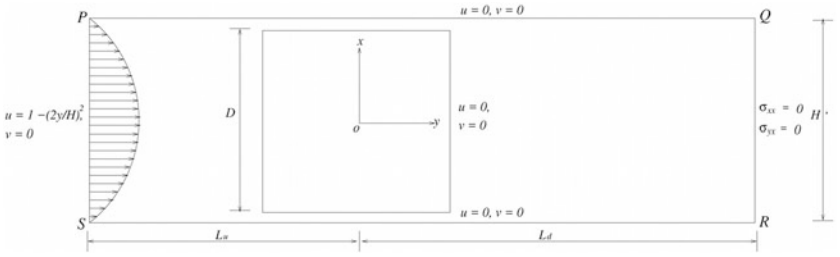

Fig. 1 Problem set-up for flow past a stationary square cylinder at high blockage ($B/H = 0.9$)

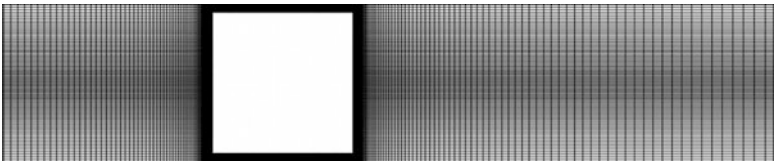

Fig. 2 Finite-element mesh with 90,460 nodes and 89,472 bilinear quadrilateral elements

3.2 The Finite-Element Mesh

Truncated finite-element mesh for the problem is shown in Fig. 2. The mesh consisting of 90,460 nodes and 89,472 bilinear quadrilateral elements is structured, non-uniform and has three blocks. The cylinder is placed in the central block. A total of 384 nodes are used to define the cylinder surface which makes an extremely fine mesh in the central block.

4 Validation and Mesh Convergence Study

4.1 Validation with Earlier Studies

A successful validation study in terms of drag coefficient (C_d) and normalized bubble length (L/D) has been performed for flow around a square cylinder at $Re = 40$ and $B = 0.067$. Validation with [11] has been tabulated in Table 1 with a maximum deviation of 2.24% obtained for C_d.

4.2 Mesh Convergence Test

To finalize the size of the mesh to be used for the optimized solution, a mesh convergence study has also been performed on several meshes. Table 2 lists two meshes M1 and M2 where M2 has approximately twice as many nodes and elements as M1. The convergence study has been studied at $Re = 100$ and $B = 0.9$. It is noticeable that the results for both the meshes do not vary significantly. Thus, mesh M1 is adequate to be used for the present computations.

Table 1 Validation study for flow past a square cylinder at zero incidence

Studies	C_d	L/D
[11]	1.8990	2.7000
Present	1.8565	2.7348
Deviation (%)	2.24	1.3

Table 2 Mesh convergence study for flow past a highly confined square cylinder at $Re = 100$

Mesh	Nodes	Elements	Equations	N_t	C_d
M1	90,460	89,472	267,618	96	661.012573
M2	173,776	172,368	516,013	162	661.163879

5 Results

5.1 Development of Steady Separation Bubble with Re

Development of the steady separation bubble is determined by streamline contour plots. For $B = 0.9$, Fig. 3a–e presents the streamline contours at $Re = 15$, 20, 30, 40 and 62, respectively. It is noteworthy that at highly blocked flow ($B = 0.9$), wake formation initiates directly from the sharp trailing edges of the square cylinder unlike from base ($\theta = 180°$) at low blockage ($B = 0.01$) [12]. For the present case, wake formation with two counterclockwise eddies initiates at $Re = 15$ (Fig. 3a). With an increase in Re, the wake bubbles expand and elongate (Fig. 3b–d) and then sheds at $Re = 62$ (Fig. 3e). Thus, $Re = 62$ marks the onset of unsteadiness in the highly blocked flow around a square cylinder.

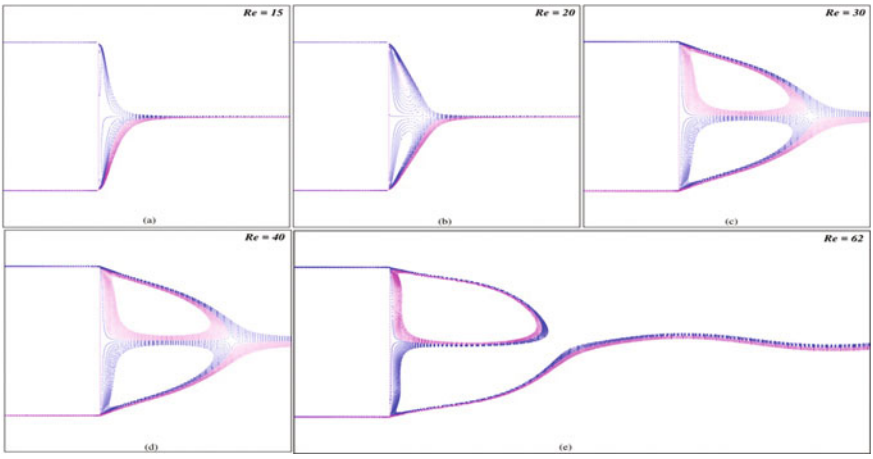

Fig. 3 Bubble separation and its development with Reynolds number for $15 \leq Re \leq 62$

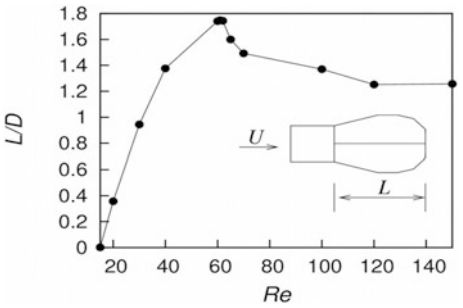

Fig. 4 Variation of eddy length with Re

5.2 *Variation of Eddy Length with* Re

Eddy length is the stream-wise distance of wake stagnation (saddle) point from the backward stagnation point on the cylinder. *L/D–Re* curve (Fig. 4) shows a variation of wake length with *Re*. In accordance with the result obtained in Sect. 5.1, *L/D* increases in the steady regime ($15 \leq Re \leq 61$) and decreases in the unsteady flow regime ($Re \geq 62$). The onset of unsteadiness is accompanied by the sudden drop in the eddy length.

5.3 *The Onset of Steady Flow Separation*

The vorticity distribution on the cylinder surface is used to determine critical *Re* and exact point of flow separation on the surface of the cylinder. Figure 5 shows ω–θ plot for $Re = 7$–11. Only one crossover point at $\theta = 180°$ in the ω–θ plot (Fig. 5) is an evidence of attached flow for $Re < 8$. Flow separation initiates at $Re \approx 8$; $\theta = 136.8°$, where the plot cuts the zero vorticity line even number of times (regions A, B). These bubbles are very small and reattaches with the surface of cylinder mush ahead of the base point.

5.4 *Variation of Drag Width* Re

The dependence of drag coefficient on *Re* is shown in Fig. 6. As expected, drag continues to fall in the entire regime. In the present study, the drag values are quite high (of the order of magnitude 10^3) unlike 1 for unconfined flow [12]. The decrease in C_d is attributed to the increasing pressure recovery at the cylinder base (Fig. 7). The variation of C_{dp} and C_{dv} are nearly identical while the pressure drag is more significant.

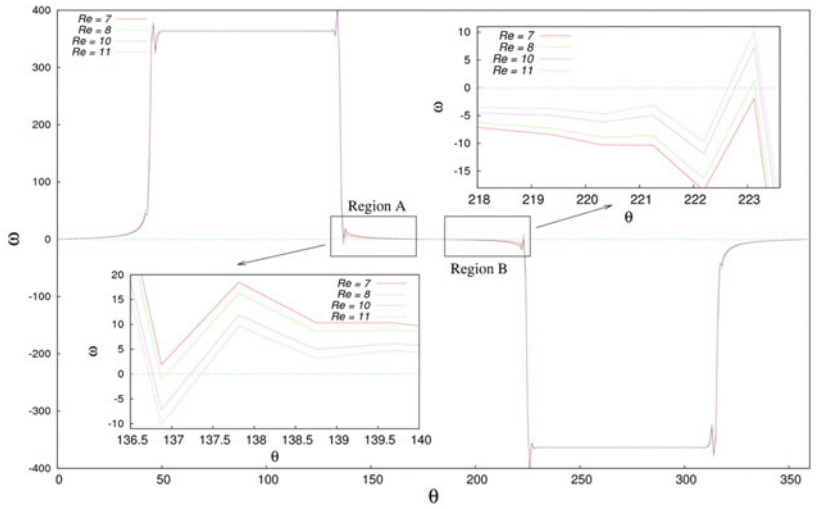

Fig. 5 Flow past a stationary square cylinder at $B = 0.9$: variation of surface vorticity distribution for $7 \leq Re \leq 11$. The insets are the close-up of regions A, B. The circumferential angle (θ) is measured counter-clockwise from forward stagnation point

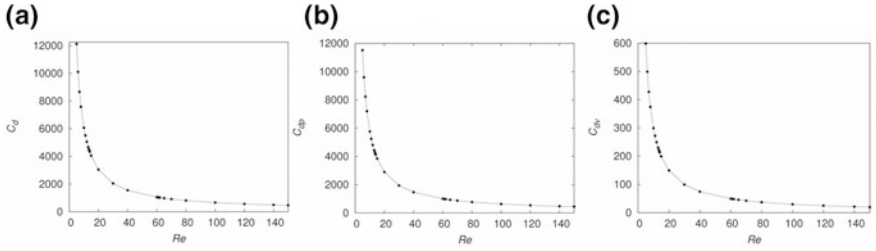

Fig. 6 Variation of C_d with Re: **a** total drag, **b** pressure drag and **c** viscous drag

5.5 *Surface Pressure Distribution*

Surface pressure (C_p) distribution for the lower half of the cylinder is shown in Fig. 7 at different Re between 5 and 150. A very large value of C_p is observed at low Re. C_p remains almost constant on front and the rear edge of the cylinder while decreases gradually on the lateral edge. A very narrow negative pressure region is observed near $\theta = 135°$ for all Re.

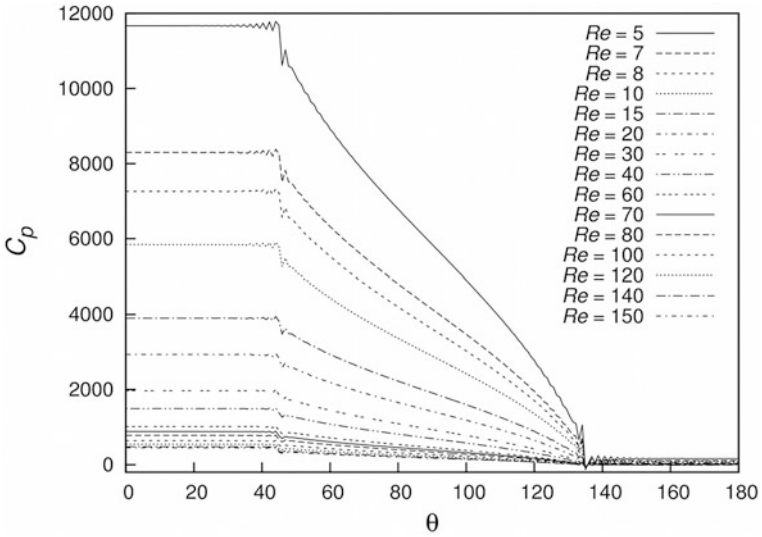

Fig. 7 Variation of C_p along the lower half the cylinder with θ

5.6 The Flow

The onset of unsteadiness obtained at $Re = 62$ is reconfirmed with the help of vorticity contours (Fig. 8). At $Re = 61$, the flow is steady as there is no undulation in the downstream flow. While at another representative Re of 62, 70, 100, 120 and 150, the disturbance in the flow is clearly observed and alternate vortex shedding from top and bottom of the cylinder starts. The existence of additional vortices on the lateral walls is also observed. The flow is periodic in the unsteady regime (suggested by figure '8' in C_d–C_l phase plots).

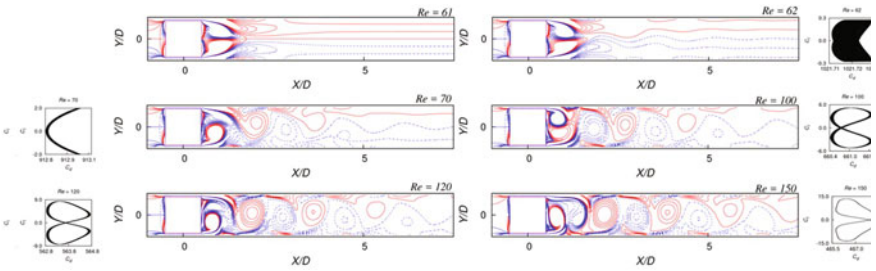

Fig. 8 Flow past a stationary square cylinder at $B = 0.9$: vorticity contours for $62 \leq Re \leq 150$. The respective C_d–C_l phase plots are shown alongside each contour

6 Conclusions

Results have been presented for flow past a stationary square cylinder for $5 \leq Re \leq 150$ at $B = 0.9$. It is found that flow remains steady for $Re < 62$. The wake formation starts at Re = 15. *L/D–Re* curve depicts a non-linear variation of wake length in steady flow regime. This is in contrast with the linear profile of *L/D–Re* for low and moderate blockage flow problems in the steady flow regime. Drag is significantly higher in confined flow (Order of 10^3) as compared to unconfined flow. Drag decreases continuously due to pressure recovery at the rear end of the cylinder. Flow becomes unsteady at $Re = 62$. It is seen that vortices generate at the cylinder surface get diffuse into the vortices on both walls due to confinement and 2S mode of vortex shedding is observed in the downstream region. Phase plots show the quasi-periodic nature of flow at $Re = 62$ and periodic for $Re = 70$, 100, 120 and 150.

References

1. Davis RW, Moore EF, Purtell LP (1984) A numerical-experimental study of confined flow around rectangular cylinders. Phys Fluids 27(1):46–59
2. Sohankar A, Norberg C, Davidson A (1996) Low-Reynolds-number flow around a square cylinder at incidence: study of blockage, onset of vortex shedding and outlet boundary condition. Int J Numer Method Fluids 26(1):39–56
3. Sharma A, Eswaran V (2004) Effect of channel confinement on the two-dimensional laminar flow and heat transfer across a square cylinder. J Numer Heat Transf 47(1):79–107
4. Kumar B, Mittal S (2006) Effect of blockage on critical parameter for flow past a circular cylinder. Int J Numer Meth Fluids 50(8):987–1001
5. Patil P, Tiwari S (2008) Effect of blockage ratio on wake transition for flow past a square cylinder. Fluid Dyn Res 40(11–12):753–778
6. Suzuki H, Inoue Y, Nishimura T, Fukutani K, Suzuki K (1993) Unsteady flow in a channel obstructed by square rod (criss-cross motion of vortex). J Heat Fluid Flow 14(1):2–9
7. Sahin M, Owens RG (2004) A numerical investigation of wall effects up to high blockage ratios on two-dimensional flow past a confined circular cylinder. Phys Fluid 16(5):1305–1320
8. Sen S, Mittal S, Biswas G (2009) Steady separated flow past a circular cylinder at low Reynolds numbers. J Fluid Mech 620:89–119
9. Verma A, Saha AK, Behra S (2017) Characteristics of two-dimensional flow past a square cylinder placed in a channel with high blockage. Fluid Mech Fluid Power Contemp Res 115–123
10. Tezduyar TE, Behr M, Mittal S, Liou J (1992) A new strategy for finite-element computations involving moving boundaries and interfaces—the DSD/ST procedure: II. Computation of free-surface flows, two-liquid flows, and lows with drifting cylinders. Comput Methods Appl Mech Eng 94:353–371
11. Paliwal B, Sharma A, Chhabra RP, Eshwaran V (2003) Power law fluid flow past a square cylinder: momentum and heat transfer characteristics. Chem Eng Sci 58:5315–5329
12. Sen S, Mittal S, Biswas G (2011) Flow past a square cylinder at low Reynolds numbers. Int J Numer Meth Fluids 67(9):1160–1174